RSC Advances

PAPER

View Article Online
View Journal | View Issue

Cite this: *RSC Adv.*, 2017, **7**, 42606

Enhanced optical confinement of dielectric nanoparticles by two-photon resonance transition†

Aungtinee Kittiravechote, Anwar Usman,‡ Hiroshi Masuhara* and Ian Liau *

Received 30th May 2017
Accepted 28th August 2017

DOI: 10.1039/c7ra06031a

rsc.li/rsc-advances

Despite a tremendous success in the optical manipulation of microscopic particles, it remains a challenge to manipulate nanoparticles especially as the polarizability of the particles is small. With a picosecond-pulsed near-infrared laser, we demonstrated recently that the confinement of dye-doped polystyrene nanobeads is significantly enhanced relative to bare nanobeads of the same dimension. We attributed the enhancement to an additional term of the refractive index, which results from two-photon resonance between the dopant and the optical field. The optical confinement is profoundly enhanced as the half-wavelength of the laser falls either on the red side, or slightly away from the blue side, of the absorption band of the dopant. In contrast, the ability to confine the nanobeads is significantly diminished as the half-wavelength of the laser locates either at the peak, or on the blue side, of the absorption band. We suggest that the dispersively shaped polarizability of the dopant near the resonance is responsible to the distinctive spectral dependence of the optical confinement of nanobeads. This work advances our understanding of the underlying mechanism of the enhanced optical confinement of doped nanoparticles with a near-infrared pulsed laser, and might facilitate future research that benefits from effective sorting of selected nanoparticles beyond the limitations of previous approaches.

Introduction

Optical trapping of microscopic objects with a focused continuous wave (cw) laser beam is a mainstream tool to manipulate microscopic particles in solutions. Despite its widespread applications in physical,[1,2] materials,[3] and life[4–6] sciences, effective trapping of particles in the nanometre scale has been demonstrated only with limited success.[7,8]

In comparison with metallic nanoparticles comprising gold[9,10] or silver[11,12] the polarizability of dielectric nanoparticles of a comparable dimension is much smaller. As a result, optical manipulation of dielectric nanoparticles remains challenging.[13] Towards this end, numerous strategies have been attempted aiming either to decrease the pushing (scattering, absorption and temporal) force, or to increase the trapping (gradient) force.[14–19] For instance, a near-infrared (NIR) pulsed laser was employed as a trapping laser to minimize the scattering and absorption forces;[14] the temporal force was further decreased with a laser of a long pulse-width.[15] On the other hand, the trapping force can be increased by maximizing the gradient of the optical field; this is achieved mainly by (i) using a high numerical-aperture (NA) objective lens, (ii) creating a large optical field in the near field,[14] or (iii) utilizing the intense optical field associated with a ultrashort pulsed laser.[16]

Distinct from these approaches, it is possible to boost the gradient force by increasing the real part of the polarizability through optical resonance. This idea has been demonstrated on trapping doped dielectric nanoparticles, whose effective polarizability is increased as a result of optical resonance between the dopant and the optical field of the trapping laser.[17–19]

More recently, multiphoton process have been proposed and realized as a novel means to facilitate optical manipulation of dielectric nanoparticles.[20–25] In particular, we employed a picosecond (ps)-pulsed NIR laser to trap doped dielectric nanobeads with the half-wavelength of the laser falling within the absorption band of the dopant. Distinct from most preceding work that addressed mainly the stiffness of the optical trap, we concerned particularly the enhanced ability to confine nanobeads near the laser focus. Our result indicates that two-photon resonance between the intense optical field of the pulsed laser and the dopant leads to an additional term in the effective refractive index of nanobeads, thereby contributing to enhanced optical confinement.[21]

In general, the polarizability and the optical cross-section (scattering and absorption) of an object depend on the frequency of the optical field that interacts with the object. Accordingly, the optical force exerting on the object at the laser focus should depend also on the frequency of the optical field.[17,18] This spectral dependence of the optical force is

Department of Applied Chemistry, Institute of Molecular Science, National Chiao Tung University, Hsinchu, Taiwan. E-mail: ianliau@mail.nctu.edu.tw; masuhara@mail.nctu.edu.tw

† Electronic supplementary information (ESI) available. See DOI: 10.1039/c7ra06031a

‡ Current address: Department of Chemistry, Faculty of Science, Universiti Brunei, Darussalam, Brunei.

expected to be particularly profound as the optical field is near resonant with the object to be trapped. Specifically, the gradient force scales with the real part of the polarizability whereas the scattering and the absorption forces depend on the optical cross-section thereby increasing near the resonance. Since the trapping and the counteracting repulsive forces both depend on the optical frequency, the efficiency of optical trapping can be maximized by optimizing the resonance between the optical field of the trapping laser and the object to be confined. This can be achieved through tuning either the wavelength of available near-infrared (NIR) adjustable laser sources or the offsets of material absorption maximum relative to the laser wavelength *vice versa*. This deduction should be applicable to not only single-photon but also two-photon resonance.

In this work, we investigated optical confinement of dielectric nanobeads doped with varied dyes with their absorption maximum exhibiting varied offsets relative to the half-wavelength of a NIR pulsed laser (termed the "trapping laser" hereafter). We particularly compared the confinement of doped nanobeads relative to their bare counterparts of the same dimension. We showed that optical confinement of doped nanobeads was significantly enhanced as the half-wavelength of the pulsed laser (FWHM 7 ps, 1064 nm) fell either on the red side, or slightly away from the blue side, of the absorption band of the dopant, whereas the ability of confinement decreased significantly as the half-wavelength of the laser located either at the peak, or on the blue side, of the absorption band of the dopant. In contrast, the spectral dependence of the optical confinement was insignificant as a continuous-wave (cw) laser of the same wavelength was employed. We attributed these observations to the dispersively shaped polarizability. This work advances our understanding of the mechanism of enhanced confinement mediated with two-photon resonance, and may shed light on future research that benefits from effective sorting of selected nanoparticles beyond the limitations of previous approaches.

Experiment

Reagents and sample preparation

Polystyrene nanobeads (Polybead, dia. 100 and 200 nm, 2.5% solids; Polysciences) and dye-doped nanobeads with maximal absorption at 505 nm (TransFluoSpheres, dia. 100 nm, 2% solids; Invitrogen), 532 nm (Fluoresbrite, dia. 100 nm, 2.5% solids; Polysciences), 543 nm (FluoSpheres, dia. 100 nm, 2% solid; Invitrogen), and 558 nm (Sphero, dia. 200 nm, 1% solids; Spherotech) were used as received. Note that 200 nm doped nanobeads with absorption maximum at 558 nm were used in this work because doped nanobeads of 100 nm in diameter were not commercially available. To avoid an elevation of temperature induced by NIR absorption of water,[26] heavy water (D_2O, 99.9 atom% D; Aldrich) was used throughout this work.

We suspended nanobeads of indicated types to a particle density 3.82×10^{13} and 1.22×10^{12} particles per ml for beads of a diameter 100 and 200 nm, respectively. Before experiments, we filled the colloidal solution in a sample cell assembled from a silicon chamber (diameter 2 cm, thickness 1 mm; EMS) sandwiched between two cover-glass plates (EMS).

Optical setup

We performed experiments on a setup modified from an inverted optical microscope (Eclipse Ti; Nikon).[21] Briefly, a pulsed laser (1064 nm, FWHM 7 ps, 76 MHz; PicoTran, High-Q Laser), or a cw laser (1064 nm; DPSSL, Changchun New Industries), was employed for optical trapping. The laser beam was first expanded and collimated using a telescope, directed to the back port of the microscope, and then focused with an objective lens (60X, NA 0.95; PlanApo; Nikon). A CCD camera (Wat-902H-1/2″; Watec) was mounted on the video port of the microscope to image optically confined nanobeads, which were illuminated by a halogen lamp through a condenser lens (NA 0.52). To minimize photo excitation by the illumination light, we selected only the red portion of the illumination with a band-pass filter (HQ 735/75; Chroma). We placed also a short-pass filter (FES 900; Thorlabs) and a band-pass filter (FB 700-10; Thorlabs) before the CCD to reject the Rayleigh scattering and the two-photon emission produced from the trapping laser. As a result, the images captured by the CCD (frame rate thirty images per second) were produced exclusively from the scattering of light with the illumination of the condenser lamp.

Image acquisition and analysis

As the intensity of scattering light scales with the number of particles,[27] we accordingly estimated the number of particles confined near the focus by determining the intensity of the image near the laser focus. We analysed the images and extracted the scattering intensity of a region of interest (16 $pixel^2$, equivalent to approximately 0.39 μm^2) that encompassed either the laser focus, or a region not illuminated by the laser (the background), with freeware (ImageJ, 1.46 m; Wayne Rasband; National Institutes of Health).

Absorption and emission spectra of varied colloidal solutions

We first measured the steady-state absorption spectra of a colloidal solution that comprised nanobeads with the dopant dyes of varied types. As shown in Fig. 1(a), the absorption spectra of these solutions exhibited a maximum approximately at 505 (blue), 532 (green), 543 (orange) and 558 (pink) nm. We noted that the doped-505 nanobeads comprised two dopants with absorption bands centred around 505 nm and 540 nm, respectively, with the former about twice stronger; we hence assume that the dopant with absorption at 505 nm dominates. Throughout this work, we denote the solutions by the wavelength of maximal absorption. As also shown in the same figure, the half-wavelength of the NIR laser (black arrow) located on the red tail (doped-505), at the peak (doped-532) and within the blue side (doped-543 and doped-558) of the absorption band of the indicated colloidal solutions. We characterized also the emission spectra of these colloidal solutions with an excitation wavelength of 532 nm; as shown in Fig. 1(b), none of these dopants produced discernible emission within the window of the band pass filters (700 ± 5 nm; the grey bar in Fig. 1(b))

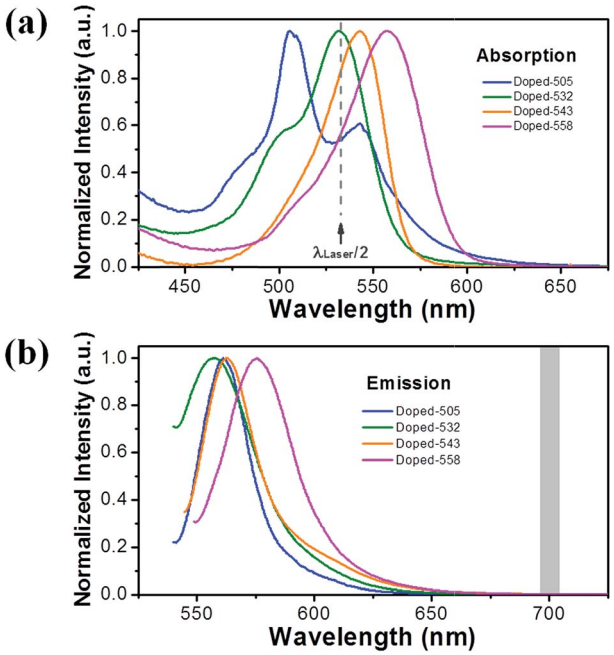

Fig. 1 (a) The absorption and (b) emission spectra of varied colloidal solutions prepared in heavy water: doped-505 (blue), doped-532 (green), doped-543 (orange), and doped-558 (pink). The black arrow and the dashed line in (a) show the half-wavelength of the trapping laser whereas the grey bar in (b) indicates the spectral window of detection of the CCD, selected by the assorted filters.

placed in front of the camera. We thus expect that the fluorescent emission of these dopants had little contribution to the image acquired by the CCD. Consequently, the images acquired by the CCD were produced exclusively from the scattering of light from the illumination of the condenser lamp. We accordingly attributed the scattering intensity (after background subtraction) of the images to the ability of optical confinement.

Results

To investigate whether the enhanced optical confinement of dielectric nanoparticles depended on optical resonance, we employed a pulsed laser ($\lambda = 1064$ nm; average power 400 mW, measured at the laser focus) to confine nanobeads with varied dopant dyes. Fig. 2(a) displays the scattering image (and the corresponding line profile) acquired on doped (left) and undoped (right) nanobeads of the same dimension whereas Fig. 2(b) shows the intensity (averaged over two minutes) determined from a region near the focus. As described, the fluorescence signals have been excluded, the scattering intensity hence served as an indicator of the number of particles confined at the laser focus.

As shown from Fig. 2(b), the scattering intensity determined on bare nanobeads of either dimension (grey bars) is slightly greater than the background (dashed line). Such increase in the scattering intensities relative to the background implied an effective confinement of bare nanobeads with the ps-pulsed NIR

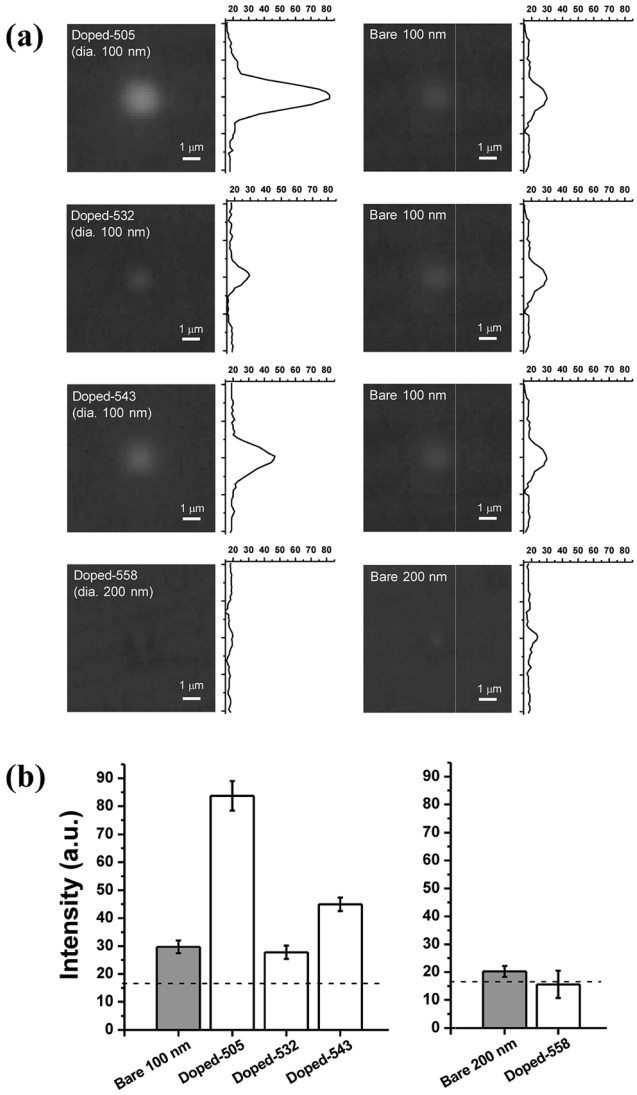

Fig. 2 The dependence of optical confinement of dielectric nanobeads on the wavelength of pulsed laser near two-photon resonance with an average power of 400 mW at the laser focus (a) the scattering image (and its corresponding line profile) acquired on doped nanobeads (left) and on undoped nanobeads (right) for 100 nm- and 200 nm-sized beads (b) the averaged intensity with its fluctuation observed for 2 minutes for (left) 100 nm- and (right) 200 nm-sized beads. Dash line denotes the background intensity.

laser.[27] Furthermore, the scattering intensity determined on doped-505 and doped-543 nanobeads was significantly greater than that on bare nanobeads of the same dimension; in contrast, the scattering intensity determined on doped-532 and doped-558 nanobeads was comparable (doped-532) or even slightly smaller (doped-558) relative their undoped counterpart of the same dimension (Fig. 2(b)). These results indicate that the confinement of nanobeads exhibited a distinct dependence on the spectral property of the dopants of nanobeads when a ps-pulsed NIR laser was used.

For comparison, we employed a cw laser of the same wavelength and averaged power to confine nanobeads. As shown in Fig. 3, each test exhibited a greater intensity relative to the

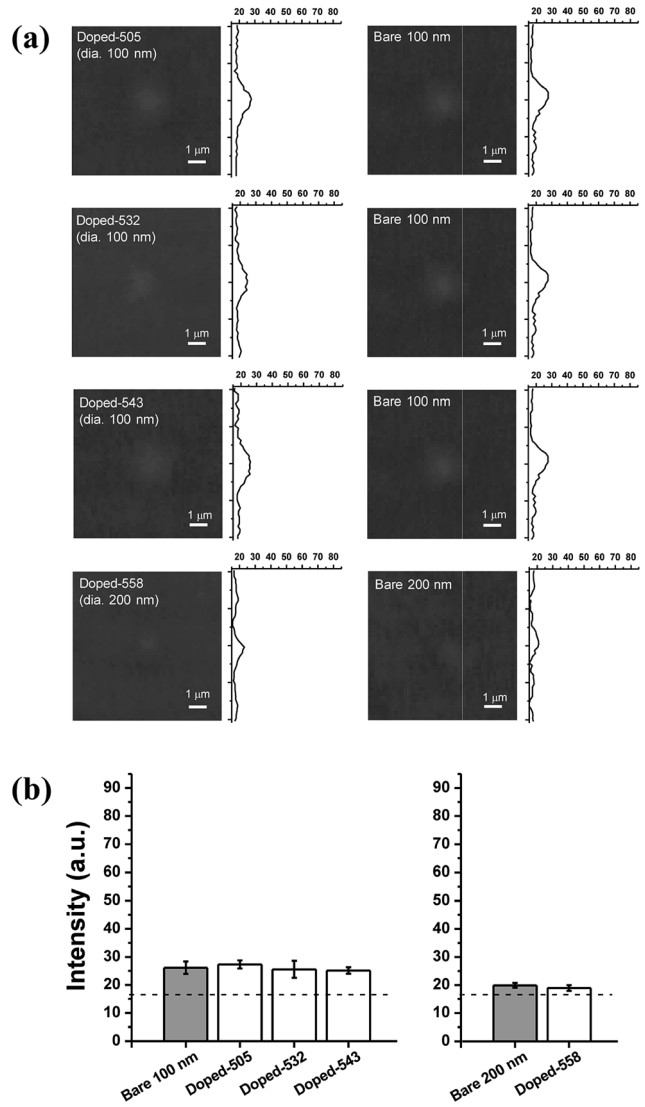

Fig. 3 The independence of optical confinement of dielectric nanobeads on the wavelength of cw laser with an average power of 400 mW at the laser focus (a) the scattering image (and its corresponding line profile) acquired on doped nanobeads (left) and on undoped nanobeads (right) for 100 nm- and 200 nm-sized beads (b) the averaged intensity with its fluctuation observed for 2 minutes for (left) 100 nm- and (right) 200 nm-sized beads. Dash line denotes the background intensity.

background; such result indicates an effective confinement of nanobeads with the NIR cw laser. However, in contrast to the results obtained with the pulsed laser, the scattering intensity determined on doped nanobeads was comparable to their undoped counterparts of the same dimension regardless of the spectral property of dopants when a cw laser was employed.

As described, 200 nm doped nanobeads with absorption maximum at 558 nm were used in this work because doped nanobeads of 100 nm in diameter were not commercially available. In order to highlight the contribution of dopants, while minimizing that of the particle size, to optical confinement, we defined the enhancement factor as the ratio of the scattering intensity (after subtracting background) determined

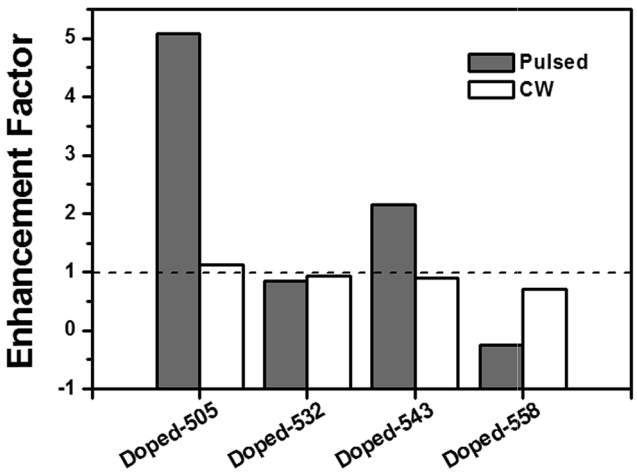

Fig. 4 Comparison of enhancement factor to confine varied dielectric nanobeads through the employment of either pulsed or cw laser with the same wavelength and averaged power of 400 mW at the laser focus (dash line represents the enhancement factor of unity).

on doped nanobeads relative to that on undoped nanobeads of the same dimension. According to such definition, an enhancement factor greater than unity indicates that the dopant enhanced the optical confinement whereas a factor comparable to, or less than one, indicates that doping had little effect or even deteriorated the ability of optical confinement.

Fig. 4 summarized a comparison of the enhancement factors determined with the pulsed (grey bars) with that determined using the cw (white bars) laser. When the pulsed laser was employed, the enhancement factor varied significantly among nanobeads with varied dopant dyes; the enhancement factor is significantly greater than unity (doped-505 and doped-543), comparable to unity (doped-532), or less than one (doped-558). These collective results show that the confinement factor was strongly modulated by dopants of varied spectral properties. In specific, the optical confinement of doped nanobeads is profoundly enhanced when the half-wavelength of the pulsed laser (1064 nm/2) located either on the red tail of absorption band (doped-505) or slightly away from the blue side of the absorption band (doped-543) whereas the enhancement was insignificant when the half-wavelength of pulsed laser matched the absorption peak (doped-532), or the half-wavelength of laser fell within the blue side of the absorption band (doped-558). Notably, such spectral modulation in the confinement factor was insignificant when the cw laser was employed (white bars, Fig. 4).

Discussion

In this work, we examined spectral dependence of the optical confinement of nanobeads using a pulsed or a cw laser. Our results specifically show that the enhancement factor depended strongly on the spectral properties of the dopants when the ps-pulsed NIR laser was employed (grey bars, Fig. 4). As the half-length of the ps-pulsed NIR laser fell within the absorption bands of the dopants (Fig. 1(a)), two-photon resonance is hence

energetically possible. We accordingly suggested that such distinct spectral dependence of the enhancement factor was medicated by two-photon resonance between the optical field of the ps-pulsed NIR laser and the dopants. In contrast, the cw NIR laser under our experimental condition was unlikely to fulfil the requirement of photon flux to induce two-photon resonance. Consistent with the deduction, the enhancement factors are comparable to unity regardless of dopants of varied type when the cw laser was employed (white bars, Fig. 4).

To consolidate our deduction, we explored also how the enhancement factor depended on the laser power. The results show that the enhancement factors of the confinement of doped-505 (blue) and doped-543 (orange) nanobeads increased approximately linearly with the laser power when the NIR pulsed laser was employed (Fig. 5). We note that the confinement efficiency of undoped nanoparticles increases linearly with the laser power.[21] As the confinement efficient of the enhancement factor was defined as the ratio of the scattering intensity determined on doped nanobeads relative to that on undoped nanobeads of the same dimension, an increase of the enhancement factor with the laser power indicates that nonlinear optical interaction plays a dominant role for the enhanced optical confinement of doped-505 and doped-543. Conforming to the result displayed in Fig. 4, the enhancement factor did not vary significantly with the power of the laser (doped-532, green), or even decreased slightly with the increasing laser power (doped-558, pink). As a negative control, we repeated the experiments using a cw laser. As expected, the enhancement factors observed on nanobeads of all types did not vary significantly with the laser power, which is consistent with our deduction that the use of a cw laser does not contribute the multiphoton mediated optical conferment.

With these results taken together, we suggested that the spectral dependence of the enhancement factor was caused by the spectral dependence of the optical polarizability. To elucidate the mechanism underlying our observation, we consider light-matter interaction. As the wavelength of trapping laser (λ = 1064 nm) is significantly greater than the dimension of the nanobeads (dia. = 100 or 200 nm), it is hence valid to consider these nanobeads as a Rayleigh particle, and the light-matter interaction between the optical field and these nanobeads can be approximated within the scheme of dipolar interaction.[28] Following the line, the trapping force acting on the sphere is gradient force, which can be expressed as[18]

$$\vec{F}_{\mathrm{grad}} = \frac{\mathrm{Re}(\alpha)}{cn_{\mathrm{m}}\varepsilon_0}\vec{\nabla}\, I, \tag{1}$$

where α is the polarizability of the sphere, n_{m} the refractive index of the medium, ε_0 the dielectric constant, and I the intensity of the optical field. The polarizability of the sphere is related to the dielectric constant of the medium (ε_{m}), the diameter of the sphere (d), and the ratio between the refractive index of the sphere (n_{s}) and the medium (n_{m}), $m = n_{\mathrm{s}}/n_{\mathrm{m}}$, and hence can be expressed as

$$\alpha = 4\pi\varepsilon_{\mathrm{m}}\left(\frac{d}{2}\right)^3\left(\frac{m^2-1}{m^2+2}\right). \tag{2}$$

The pushing force acting on the sphere comprises two terms, the scattering force,

$$\vec{F}_{\mathrm{scat}} = \hat{k}\frac{4\pi^3 n_{\mathrm{m}}}{c\varepsilon_0{}^2\lambda^4}|\alpha|^2 I, \tag{3}$$

and the absorption force

$$\vec{F}_{\mathrm{abs}} = \hat{k}\frac{2\pi}{c\varepsilon_0\lambda}\mathrm{Im}(\alpha)I. \tag{4}$$

We first evaluate the contribution of the scattering force relative to the gradient force in the Rayleigh regime (more detail in the ESI†). According to the preceding equations, the gradient force scales linearly with the real part of the polarizability (eqn (1)) whereas the scattering force scales with the squared polarizability (eqn (3)). As the polarizability of a sphere is proportional to the volume of the sphere (eqn (2)), the scattering force is small in comparison with the gradient force when considering small Rayleigh particles.[18] In general, the imaginary part of the polarizability might contribute additional terms to the scattering force. However, as the scattering force scales with the squared polarizability (and hence the squared volume), we argue that the contribution to the scattering force from the imaginary polarizability is also small relative to the gradient force as long as the particle is in the Rayleigh regime regardless

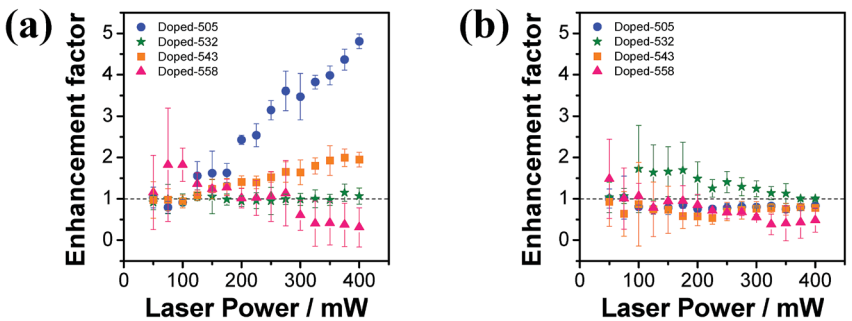

Fig. 5 The power dependence of enhancement factor to confine dye-doped dielectric nanobeads through the employment of (a) pulsed laser and (b) cw laser. Blue circles: doped-505 beads; green stars: doped-532 beads; orange squares: doped-543 beads; pink triangles: doped-558 beads; dash line: enhancement factor of 1. The results are averaged by triply repeated data set.

of non-resonant or resonant conditions. We hence neglect the scattering force.

We proceeded to evaluate the contribution of the gradient force relative to the absorption force, which scales with the real (eqn (1)) and the imaginary part (eqn (4)) of the polarizability, respectively. To this end, we assessed how the real and the imaginary parts of the polarizability vary with the optical frequency according to the classical model of electron oscillation in a way similar to that reported by Kendrick and coworkers.[18] As illustrated in Fig. 6, the imaginary part is a Lorentzian centered at the maximum of the absorption spectrum (black curve) whereas the real part exhibits a dispersive profile that crosses zero at the maximum of the absorption spectrum (red curve). More importantly, the result shows clearly that the relative contribution of the gradient force and the absorption force varies significantly with the optical frequency according to the relative magnitude of the real polarizability ($\mathrm{Re}(\alpha)$) and the imaginary counterpart ($\mathrm{Im}(\alpha)$). Moreover, such spectral dependence varies most profoundly near the resonance. Although the conclusion was deduced within the context of single-photon resonance, we assume that it applies to the case of two-photon resonance.

In this work, a 1064 nm pulsed laser was employed to trap doped nanobeads that have profound absorption in the visible range. As describe, we have verified the generation of two-photon fluorescence on exciting the doped nanobead with the 1064 nm pulsed laser.[21] This result indicates that two-photon resonance between the optical field of the laser and the dopant was fulfilled.

Although the two-photon absorption spectrum of dopants are generally unknown, we assume that the spectral profile of the two-photon absorption spectrum is similar to that of the single-photon absorption spectrum except that the wavelength scale is scaled by a factor of two. Similarly, the complex polarizability in the two-photon regime is approximated with that in the single-photon regime after multiplying the wavelength scale by a factor of two, and exhibits a spectral profile similar to that displayed in Fig. 6 (except the doubled wavelength scale).

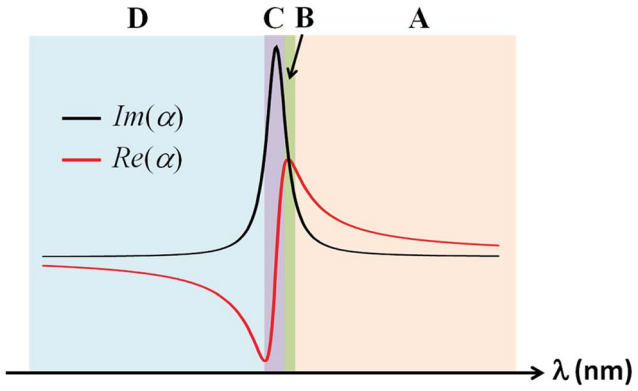

Fig. 6 Spectral dependence of the dispersively shaped real part of the complex polarizability ($\mathrm{Re}(\alpha)$) and the Lorentzianly shaped imaginary counterpart ($\mathrm{Im}(\alpha)$) shown in red and black curves. The regions highlighted with different colors represent spectral regions with distinct relative magnitudes between the real and the imaginary part of the complex polarizability.

To facilitate discussion, we highlighted four distinct spectral regions according to the relative magnitudes of the real and the imaginary parts of the complex polarizability. As shown in Fig. 6, the magnitude of the real part of the complex polarizability is greater than that of the imaginary part as the wavelength of the laser is near and above the maximum of the two-photon absorption band of the doped nanobeads (Region A); we thus expect to observe an enhanced trapping in this spectral region. As the wavelength of the laser is tuned toward the absorption maximum, the magnitude of the real part becomes comparable with that of the imaginary part (Region B); there is thus no enhancement in this spectral region. Below the region, the magnitude of the real part becomes less than that of the imaginary part (Region C); we expect that particles would be pushed predominantly along the direction of the absorption force (the propagation direction of the laser). Finally, the magnitude of the real part becomes greater than that of the imaginary part, but in an opposite sign, as the wavelength of the laser is tuned further toward the blue side (Region D); the negative gradient force that pushes the particles outward the focus becomes dominant.

Conforming to the deduction, we observed an enhanced confinement of "doped-505 nanobeads" in which the wavelength of the pulsed laser located at the red side of the two-photon absorption band ($\lambda_{\mathrm{laser}} = 1064$ nm *vs.* $\lambda_{\mathrm{2P\text{-}Abs}} = 1010$ nm; Region A). Consistently, the enhancement of optical confinement was insignificant for "doped-532 nanobeads" whose two-photon absorption maximum coincided with the wavelength of the pulsed laser ($\lambda_{\mathrm{laser}} = 1064$ nm *vs.* $\lambda_{\mathrm{2P\text{-}Abs}} = 1064$ nm; Region B or C). Moreover, we observed a slight decrease in the efficiency of the optical confinement of "doped-558 nanobeads" in which the wavelength of the pulsed laser located at the blue side of the two-photon absorption band ($\lambda_{\mathrm{laser}} = 1064$ nm *vs.* $\lambda_{\mathrm{2P\text{-}Abs}} = 1116$ nm; Region D).

Despite the consistency, we observed an enhanced optical confinement of "doped-543 nanobeads" with the wavelength of the pulsed laser falling within the blue side of the absorption peak of the dopant ($\lambda_{\mathrm{laser}} = 1064$ nm *vs.* $\lambda_{\mathrm{2P\text{-}Abs}} = 1086$ nm). We attribute the unexpectedly increased optical confinement to the discrepancy between the true two-photon absorption spectrum of the dopant with respect to the hypothetic two-photon absorption spectrum approximated simply by multiplying the wavelength scale of the single-photon absorption spectrum by a factor of two. We note that the maximum of two-photon absorption spectrum tends to have a blue shift relative to that predicted by assuming twice of the peak of the single-photon absorption spectrum.[29] In line with this, this blue-shift of two-photon absorption maximum might cause the wavelength of the pulsed laser to locate within the red tail of the two-photon spectrum, hence leading to an enhanced confinement.

Summary

In brief, we investigate optical confinement of nanoparticles mediate by two-photon resonance. The optical confinement of

doped nanobeads varied significantly according to the offsets of their absorption maximum relative to the half-wavelength of the pulsed laser. Specifically, there is an enhanced and diminished optical confinement as the laser wavelength locates within the red or the blue tail of the two-photon absorption band, respectively, and the enhancement is negligible as the laser wavelength coincides with the two-photon absorption maximum. The general trend of this distinct spectral dependence of the optical confinement was explained with the dispersively shaped real polarizability and the Lorentzianly shaped imaginary polarizability in the context of two-photon resonance. This work advances our understanding of a novel mechanism of optical confinement mediated by two-photon resonance, and might arise new applications such as a sorting of nanoparticles based on their spectral properties.

Conflicts of interest

There are no conflicts of interest to declare.

Acknowledgements

We thank Professor Yuan-Pern Lee (National Chiao Tung University, Taiwan) for generous support, and Professor Chung-Hsuan Chen (Academia Sinica, Taiwan) for providing equipment. National Chiao Tung University, Ministry of Science and Technology, and the MOE-ATU program of Taiwan provided support to I. L. and H. M.

References

1 K. Dholakia, P. Reece and M. Gu, Optical micromanipulation, *Chem. Soc. Rev.*, 2008, **37**(1), 42–55, DOI: 10.1039/b512471a.
2 R. W. Bowman and M. J. Padgett, Optical trapping and binding, *Rep. Prog. Phys.*, 2013, **76**, 026401.
3 K.-i Yuyama, T. Sugiyama and H. Masuhara, Laser Trapping and Crystallization Dynamics of l-Phenylalanine at Solution Surface, *J. Phys. Chem. Lett.*, 2013, **4**(15), 2436–2440, DOI: 10.1021/jz401122v.
4 W.-T. Chang, H.-L. Lin, H.-C. Chen, Y.-M. Wu, W.-J. Chen, Y.-T. Lee, *et al.*, Real-time molecular assessment on oxidative injury of single cells using Raman spectroscopy, *J. Raman Spectrosc.*, 2009, **40**(9), 1194–1199, DOI: 10.1002/jrs.2261.
5 M.-C. Zhong, X.-B. Wei, J.-H. Zhou, Z.-Q. Wang and Y.-M. Li, Trapping red blood cells in living animals using optical tweezers, *Nat. Commun.*, 2013, **4**, 1768, DOI: 10.1038/ncomms2786.
6 C. Monico, M. Capitanio, G. Belcastro, F. Vanzi and F. Pavone, Optical Methods to Study Protein-DNA Interactions *in Vitro* and in Living Cells at the Single-Molecule Level, *Int. J. Mol. Sci.*, 2013, **14**(2), 3961, DOI: 10.3390/ijms14023961.
7 A. Usman, W.-Y. Chiang and H. Masuhara, Optical trapping of nanoparticles by ultrashort laser pulses, *Sci. Prog.*, 2013, **96**, 1–18, DOI: 10.3184/003685013x13592844053451.
8 A. S. Urban, S. Carretero-Palacios, A. A. Lutich, T. Lohmuller, J. Feldmann and F. Jackel, Optical trapping and manipulation of plasmonic nanoparticles: fundamentals, applications, and perspectives, *Nanoscale*, 2014, **6**(9), 4458–4474, DOI: 10.1039/c3nr06617g.
9 F. Hajizadeh and S. N. Reihani, Optimized optical trapping of gold nanoparticles, *Opt. Express*, 2010, **18**, 551–559.
10 M. J. Guffey and N. F. Scherer, All-Optical Patterning of Au Nanoparticles on Surfaces Using Optical Traps, *Nano Lett.*, 2010, **10**(11), 4302–4308, DOI: 10.1021/nl904167t.
11 J. Prikulis, F. Svedberg, M. Käll, J. Enger, K. Ramser, M. Goksör, *et al.*, Optical Spectroscopy of Single Trapped Metal Nanoparticles in Solution, *Nano Lett.*, 2003, **4**(1), 115–118, DOI: 10.1021/nl0349606.
12 L. Bosanac, T. Aabo, P. M. Bendix and L. B. Oddershede, Efficient Optical Trapping and Visualization of Silver Nanoparticles, *Nano Lett.*, 2008, **8**(5), 1486–1491, DOI: 10.1021/nl080490+.
13 K. Svoboda and S. M. Block, Optical trapping of metallic Rayleigh particles, *Opt. Lett.*, 1994, **19**, 930–932.
14 D. Erickson, X. Serey, Y.-F. Chen and S. Mandal, Nanomanipulation using near field photonics, *Lab Chip*, 2011, **11**(6), 995–1009, DOI: 10.1039/c0lc00482k.
15 W.-Y. Chiang, A. Usman and H. Masuhara, Femtosecond Pulse-Width Dependent Trapping and Directional Ejection Dynamics of Dielectric Nanoparticles, *J. Phys. Chem. C*, 2013, **117**(37), 19182–19188, DOI: 10.1021/jp404372a.
16 A. Usman, W.-Y. Chiang and H. Masuhara, Optical trapping and polarization-controlled scattering of dielectric spherical nanoparticles by femtosecond laser pulses, *J. Photochem. Photobiol., A*, 2012, **234**, 83–90, DOI: 10.1016/j.jphotochem.2011.11.015.
17 R. R. Agayan, F. Gittes, R. Kopelman and C. F. Schmidt, Optical trapping near resonance absorption, *Appl. Opt.*, 2002, **41**, 2318–2327.
18 M. J. Kendrick, D. H. McIntyre and O. Ostroverkhova, Wavelength dependence of optical tweezer trapping forces on dye-doped polystyrene microspheres, *J. Opt. Soc. Am. B*, 2009, **26**, 2189–2198.
19 C. Hosokawa, H. Yoshikawa and H. Masuhara, Enhancement of biased diffusion of dye-doped nanoparticles by simultaneous irradiation with resonance and nonresonance laser beams, *Jpn. J. Appl. Phys.*, 2006, **45**, L453–L456.
20 T. Kudo and H. Ishihara, Proposed nonlinear resonance laser technique for manipulating nanoparticles, *Phys. Rev. Lett.*, 2012, **109**, 087402.
21 A. Kittiravechote, W.-Y. Chiang, A. Usman, I. Liau and H. Masuhara, Enhanced optical confinement of dye-doped dielectric nanoparticles using a picoseconds-pulsed near-infrared laser, *Laser Phys. Lett.*, 2014, **11**, 076001.
22 W.-Y. Chiang, T. Okuhata, A. Usman, N. Tamai and H. Masuhara, Efficient Optical Trapping of CdTe Quantum Dots by Femtosecond Laser Pulses, *J. Phys. Chem. B*, 2014, **118**(49), 14010–14016, DOI: 10.1021/jp502524f.

23 L. Jauffred, A. C. Richardson and L. B. Oddershede, Three-Dimensional Optical Control of Individual Quantum Dots, *Nano Lett.*, 2008, **8**(10), 3376–3380, DOI: 10.1021/nl801962f.
24 L. Jauffred and L. B. Oddershede, Two-Photon Quantum Dot Excitation during Optical Trapping, *Nano Lett.*, 2010, **10**(5), 1927–1930, DOI: 10.1021/nl100924z.
25 C. R. Head, E. Kammann, M. Zanella, L. Manna and P. G. Lagoudakis, Spinning nanorods – active optical manipulation of semiconductor nanorods using polarised light, *Nanoscale*, 2012, **4**(12), 3693–3697, DOI: 10.1039/c2nr30515a.
26 S. Ito, T. Sugiyama, N. Toitani, G. Katayama and H. Miyasaka, Application of Fluorescence Correlation Spectroscopy to the Measurement of Local Temperature in Solutions under Optical Trapping Condition, *J. Phys. Chem. B*, 2007, **111**(9), 2365–2371, DOI: 10.1021/jp065156l.
27 C. F. Bohren and D. R. Huffman, *Absorption and Scattering of Light by Small Particles*, Wiley, New York, 1983.
28 R. S. Conroy, B. T. Mayers, D. V. Vezenov, D. B. Wolfe, M. G. Prentiss and G. M. Whitesides, Optical waveguiding in suspensions of dielectric particles, *Appl. Opt.*, 2005, **44**(36), 7853–7857, DOI: 10.1364/ao.44.007853.
29 C. Xu, W. Zipfel, J. B. Shear, R. M. Williams and W. W. Webb, Multiphoton fluorescence excitation: New spectral windows for biological nonlinear microscopy, *Proc. Natl. Acad. Sci. U. S. A.*, 1996, **93**, 10763–10768.